J|A|C|S
COMMUNICATIONS

Published on Web 03/10/2004

Nickel Oxidation States of F_{430} Cofactor in Methyl-Coenzyme M Reductase

Jennifer L. Craft,[†] Yih-Chern Horng,[‡] Stephen W. Ragsdale,[‡] and Thomas C. Brunold*,[†]

Department of Chemistry, University of Wisconsin, Madison, Wisconsin 53706, and Department of Biochemistry, University of Nebraska, Lincoln, Nebraska 68588

Received August 22, 2003; E-mail: brunold@chem.wisc.edu

Methyl-CoM reductase (MCR) catalyzes the final step of methane formation in methanogenic archaea.[1] In this process, methyl-CoM undergoes two-electron reduction with CoB to give methane and CoM−S−S−CoB. At the heart of MCR is the nickel-containing hydrocorphin cofactor F_{430}. In the crystallographically characterized, inactive forms of MCR, the cofactor is in an EPR-silent Ni(II) state.[2] While the active form of the enzyme, red1, contains a Ni(I) ion, the oxidation state of its predecessor in vitro, ox1, is a subject of intense research.[3−6] EPR and ^{14}N ENDOR studies,[3,4] together with X-ray absorption (XAS) and resonance Raman data,[5] suggested that ox1 also contains Ni(I) and that its conversion to red1 involves a hydrocorphin π-bond reduction.[5] However, a more recent XAS study demonstrated similar electron densities on nickel in ox1 and the Ni(II) state ox1-silent.[6] Here, electronic absorption (Abs), magnetic circular dichroism (MCD), and variable-temperature variable-field (VTVH) MCD are used in combination with DFT and time-dependent DFT (TD-DFT) calculations to provide new insight into MCR redox chemistry.

MCD data for ox1-silent (Figure 1) and the isolated Ni(II)F_{430} cofactor[7] are nearly identical, both consistent with high-spin $S = 1$ Ni(II) species. The TD-DFT-calculated Abs spectrum for an ox1-silent model (Ni(II)F_{430} ligated by $^{-}$S·CoM and O·Gln[2]) nicely reproduces the experimental data (Figure 2).[8] This computation reveals that the occupied Ni(II) 3d orbitals are significantly lower in energy than the hydrocorphin-based π/π^* frontier MOs, leading to the dominance of $\pi \rightarrow \pi^*$ transitions in the Abs and MCD spectra of ox1-silent (and the isolated Ni(II)F_{430} cofactor[7]).

As anticipated, MCD data for the red1 state (Figure 1) and the isolated Ni(I)F_{430} cofactor[7] are also similar, both indicative of $S = 1/2$ Ni(I). The TD-DFT-calculated Abs spectrum for a red1 model (Ni(I)F_{430} ligated by O·Gln[6]) agrees reasonably well with experimental data (Figure 2). Good agreement was also achieved between computed and experimental EPR parameters for red1 (Table S1), providing further validation of the DFT method in evaluating viable models of enzyme-bound F_{430} species. From these computations, metal ion reduction causes the Ni 3d orbitals to shift between the hydrocorphin-based HOMO and LUMO, leading to a blue-shift of the dominant $\pi \rightarrow \pi^*$ transition from 430 to 380 nm and the appearance of numerous intense MCD features in the visible/near-IR region associated with Ni 3d → hydrocorphin π^* charge-transfer transitions (Figure 1). Notably, our DFT calculations reproduce the key Abs and EPR features of red1 (and the isolated Ni(I)F_{430} cofactor;[7] see also ref 9) without incorporating a reduced hydrocorphin ring, implying that red1 is only one-electron reduced relative to ox1-silent.

Titration experiments showed ox1 to be 1−3 electrons more oxidized than red1.[5] Because hydrocorphin reduction is unnecessary to explain the spectral differences between ox1-silent and red1, we are presented with a former dilemma:[5] what electronic features distinguish ox1 and red1? Interestingly, our ox1 Abs and MCD data (Figures 1 and 2; corrected for 36% ox1-silent contributions as determined by ox1 EPR spin quantitation) are remarkably similar to those of Ni(II)F_{430} and ox1-silent. Thus, although ox1 exhibits Ni(I)-like EPR properties (Table S1),[3,4] our excited-state data appear qualitatively more consistent with a Ni(II) species.

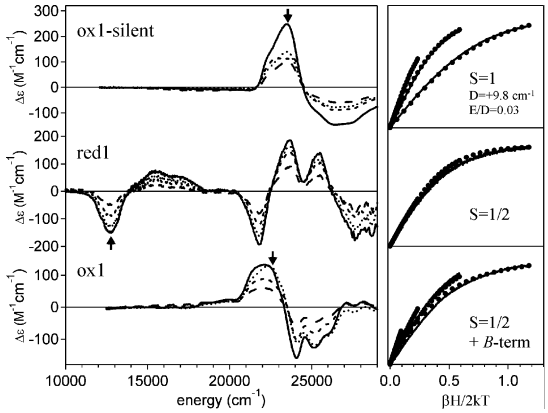

Figure 1. Left: Field-dependent 4 K MCD spectra (7, 5, 3.5, 2 T) for ox1-silent, red1, and ox1 enzymatic states. Right: VTVH MCD data (2, 4, 10, and 25 K) collected at the positions indicated by arrows in the left spectra. Both experimental (solid lines) and simulated (●) data are shown.

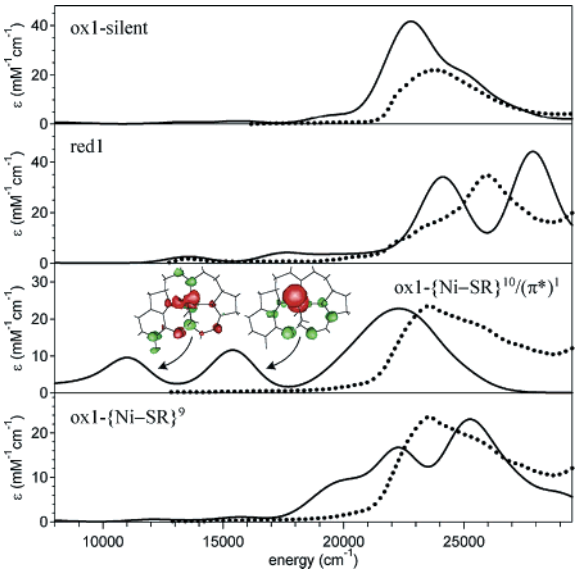

Figure 2. TD-DFT-calculated (solid) and experimental (dotted) Abs spectra.[8] Insets: EDDMs for low-energy transitions in the ox1-{Ni−SR}^{10}/(π^*)^1 spectrum. Red/green indicate loss/gain of electron density.

Previous EXAFS studies revealed that ox1 is a 6-coordinate species,[6] and cryoreduction experiments suggested that ox1-silent → ox1 conversion involves one-electron reduction.[4] Our initial computational model of ox1 was thus generated by adding an electron to our ox1-silent model. Significantly, in geometry optimizations of this model using both hybrid and pure DFT

[†] University of Wisconsin.
[‡] University of Nebraska.

10.1021/ja038082p CCC: $27.50

methods, the additional electron did not localize on the Ni(II) ion but rather on the macrocycle. In the absence of a major conformational change (as proposed for red2[10]), reduction of Ni(II)F_{430} axially coordinated by $^{-}$S·CoM is thus not expected to occur at the nickel.[11] The TD-DFT-calculated Abs spectrum for this model, termed ox1-{Ni−SR}^{10}/(π*)^1,[12] exhibits two intense low-energy features, both of which involve the singly occupied hydrocorphin π*-based MO (see electron density difference maps (EDDMs) in Figure 2, insets). The lack of corresponding features in the experimental spectrum (Figure 2) clearly argues against the presence of such a hydrocorphin radical in ox1. Moreover, while the ground-state wave function of this exchange-coupled $S = 1/2$ spin system (a multideterminantal problem) cannot be accurately described by DFT, coupling of the unpaired Ni $3d_{x^2-y^2}$ electron and the ring radical in ox1-{Ni−SR}^{10}/(π*)^1 would be expected to yield g values reminiscent of a Ni(III) $(3d_{z^2})^1$ ground state, with $g_x,g_y > g_z \approx g_e$, in obvious discrepancy with the experimental g values of 2.23, 2.17, and 2.15.[3,4] Likewise, ^{14}N hyperfine couplings, estimated from the values calculated for the ox1-silent model and an isolated hydrocorphin radical, agree poorly with experimental findings (Table S1; see Supporting Information for details). Together, our DFT and TD-DFT computations provide a strong case against this ox1 electronic description.

Biochemical evidence demonstrating that ox1 is more oxidized than red1[1,13] prompted us to test a model of ox1 obtained by one-electron oxidation of our ox1-silent model. Full DFT geometry optimization of this model led to reasonable axial bond distances[14] and afforded a {Ni−SR}^{9} species that can formally be described as Ni(II) coupled to a thiyl radical (•S·CoM). The corresponding TD-DFT-calculated Abs spectrum adequately reproduces the dominant features observed experimentally (Figure 2). As for ox1-silent, the occupied Ni(II) 3d orbitals of ox1-{Ni−SR}^{9} are calculated too low in energy to notably perturb hydrocorphin-based π/π* frontier MOs, consistent with the similar Abs and MCD spectra of ox1 and ox1-silent. Additionally, strong coupling of the unpaired Ni $3d_{z^2}$ electron and the thiyl radical in the {Ni−SR}^{9} unit would be expected to yield g values and ^{14}N hyperfine couplings (Table S1) suggestive of a Ni(I) $(3d_{x^2-y^2})^1$ ground state, with $g_z > g_x,g_y > g_e$, as observed experimentally for ox1.[3,4,15] While ox1 and ox1-silent VTVH MCD data (Figure 1) are qualitatively similar, both revealing apparent $S > 1/2$ saturation behavior, only the latter could be fit to an $S = 1$ spin Hamiltonian.[16] Attempts to fit the ox1 data for both positive and negative D values and allowing E/D to vary met with little success, ruling out that our ox1 data are dominated by an $S = 1$ minority species. Instead, the ox1 curves appear consistent with an $S = 1/2$ species (as required by EPR data[3,4]), since the observed nesting is reasonably accounted for by including a temperature-independent MCD B-term contribution. This result suggests that ox1 possesses low-lying excited states that mix with the ground state in the presence of a magnetic field,[16] which also appears inconsistent with a red1-like Ni(I) description of ox1.

Collectively, these results suggest that our ox1-{Ni−SR}^{9} model provides a reasonable description of the ox1 species. Although cryoreduction experiments were interpreted as indicating a reductive process for ox1-silent → ox1 conversion,[4] it appears that γ-irradiation actually leads to formation of a {Ni−SR}^{9} species, since removal of the σ-antibonding electron from the {Ni−SR}^{10} unit in ox1-silent could be facilitated by formation of a stable two-center/two-electron σ-bond. Due to strong coupling of the unpaired Ni $3d_{z^2}$ electron and the •S·CoM radical, the resulting $S = 1/2$ EPR signal should be unaffected by the presence of ^{33}S, consistent with experimental ox1 data.[17] Note that a similar spin-coupling scheme has been invoked to explain the EPR properties of synthetic and enzymatic {Fe−NO}^{7} systems. Detailed studies by Solomon and co-workers[18] revealed that the $S = 3/2$ ground state observed for these species arises from strong antiferromagnetic coupling between the Fe(III) center ($S = 5/2$) and NO$^-$ ($S = 1$). As the remaining three unpaired electrons reside in Fe 3d-based MOs that do not delocalize onto the NO$^-$ unit, no ^{14}N or ^{17}O hyperfine broadening of the $S = 3/2$ EPR signal is observed.

In summary, we hypothesize that ox1 is a {Ni−SR}^{9} species that can formally be described as Ni(II) coupled to a thiyl radical (•S·CoM). On the basis of the results presented here and recent XAS data,[6] this proposal is favored over the alternative Ni(III)/thiolate formulation and seems plausible in light of known nickel thiolate chemistry, which often involves redox-active sulfur ligands.[19] Further, the notion of noninnocent sulfur ligands is not new to biochemistry; e.g., sulfur-based radicals have also been proposed for thiolate compound I intermediates.[20] Notably, on the basis of DFT calculations, Pelmenschikov et al. recently proposed an ox1-like intermediate (a Ni(II)-thiolate with a nearby methyl radical) in the catalytic cycle of MCR.[21] Hence, ox1 may have mechanistic relevance beyond its identity as a red1 precursor.

Acknowledgment. This work was supported by the University of Wisconsin, The Research Corporation Award No. RI0596, NSF CAREER Grant MCB-0238530 (T.C.B.), and DOE grant DE-FG03-98ER20297 (S.W.R.). We thank Dr. Frank Neese for his help with the computational aspects of this work.

Supporting Information Available: Computational details, experimental and computed EPR parameters (Table S1), and DFT-optimized structures (Tables S2−S5) (PDF). This material is available free of charge via the Internet at http://pubs.acs.org.

References

(1) Ragsdale, S. W. In *The Porphyrin Handbook*; Kadish, K. M., Smith, K. M., Guilard, R., Eds.; Academic Press: New York, 2003; Vol. 11, p 205.
(2) Ermler, U.; Grabarse, W.; Shima, S.; Goubeaud, M.; Thauer, R. K. *Science* **1997**, *278*, 1457.
(3) Telser, J.; Horng, Y.-C.; Becker, D. F.; Hoffman, B. M.; Ragsdale, S. W. *J. Am. Chem. Soc.* **2000**, *122*, 182.
(4) Telser, J.; Davydov, R.; Horng, Y.-C.; Ragsdale, S. W.; Hoffman, B. M. *J. Am. Chem. Soc.* **2001**, *123*, 5853.
(5) Tang, Q.; Carrington, P. E.; Horng, Y.-C.; Maroney, M. J.; Ragsdale, S. W.; Bocian, D. F. *J. Am. Chem. Soc.* **2002**, *124*, 13242.
(6) Duin, E. C.; Cosper, N. J.; Mahlert, F.; Thauer, R. K.; Scott, R. A. *J. Biol. Inorg. Chem.* **2003**, *8*, 141.
(7) Craft, J. L.; Horng, Y.-C.; Ragsdale, S. W.; Brunold, T. C. *J. Biol. Inorg. Chem.* **2004**, *9*, 77.
(8) All spectra were uniformly downshifted by 5500 cm^{-1} to compensate for the tendency of B3LYP DFT to overestimate transition energies.[7]
(9) Piskorski, R.; Jaun, B. *J. Am. Chem. Soc.* **2003**, *125*, 13120.
(10) Finazzo, C.; Harmer, J.; Jaun, B.; Duin, E. C.; Mahlert, F.; Thauer, R. K.; Van Doorslaer, S.; Schweiger, A. *J. Biol. Inorg. Chem.* **2003**, *8*, 586.
(11) From our TD-DFT calculation, the excited state arising from the Ni(I) $(d_{z^2})^2(d_{x^2-y^2})^1$ electron configuration, previously believed to be the ground state of ox1,[3,4] is ∼0.9 eV (21 kcal/mol) higher in energy due to the large destabilization of the Ni $3d_{z^2}$-based MO by $^{-}$S·CoM.
(12) The superscript n in {Ni−SR}^{n} indicates the number of Ni 3d and S $3p_z$ valence electrons; e.g., for ox1-silent, $n = 10$.
(13) Rospert, S.; Bocher, R.; Albracht, S. P. J.; Thauer, R. K. *FEBS Lett.* **1991**, *291*, 371.
(14) Optimized Ni−S and Ni−O bond lengths (2.34 and 2.15 Å, respectively) are similar to those obtained by EXAFS[6] (2.40 and 2.08 Å).
(15) While a Ni(I) description was previously invoked for ox1 because similar ^{14}N hyperfine tensors were obtained for ox1 and red1,[3] it should be noted that these tensors primarily depend on the spin density in the Ni $3d_{x^2-y^2}$ orbital (singly occupied in both Ni(I) and $S = 1$ Ni(II) species).
(16) Neese, F.; Solomon, E. I. *Inorg. Chem.* **1999**, *38*, 1847.
(17) Finazzo, C.; Harmer, J.; Bauer, C.; Jaun, B.; Duin, E. C.; Mahlert, F.; Goenrich, M.; Thauer, R. K.; Van Doorslaer, S.; Schweiger, A. *J. Am. Chem. Soc.* **2003**, *125*, 4988.
(18) (a) Zhang, Y.; Pavlosky, M. A.; Brown, C. A.; Westre, T. E.; Hedman, B.; Hodgson, K. O.; Solomon, E. I. *J. Am. Chem. Soc.* **1992**, *114*, 9189. (b) Brown, C. A.; Pavlosky, M. A.; Westre, T. E.; Zhang, Y.; Hedman, B.; Hodgson, K. O.; Solomon, E. I. *J. Am. Chem. Soc.* **1995**, *117*, 715.
(19) See, for example: Kumar, M.; Day, R. O.; Colpas, G. J.; Maroney, M. J. *J. Am. Chem. Soc.* **1989**, *111*, 5974.
(20) Green, M. T. *J. Am. Chem. Soc.* **1999**, *121*, 7939.
(21) Pelmenschikov, V.; Blomberg, M. R. A.; Siegbahn, P. E. M.; Crabtree, R. H. *J. Am. Chem. Soc.* **2002**, *124*, 4039.

JA038082P